



# Characterization of a Biflaviolin Synthase CYP158A3 from *Streptomyces avermitilis* and Its Role in the Biosynthesis of Secondary Metabolites

Young-Ran Lim<sup>1</sup>, Songhee Han<sup>1</sup>, Joo-Hwan Kim<sup>1</sup>, Hyoung-Goo Park<sup>1</sup>, Ga-Young Lee<sup>2</sup>, Thien-Kim Le<sup>2</sup>, Chul-Ho Yun<sup>2</sup> and Donghak Kim<sup>1,\*</sup>

<sup>1</sup>Department of Biological Sciences, Konkuk University, Seoul 05025,

<sup>2</sup>School of Biological Sciences and Technology, Chonnam National University, Gwangju 61186, Republic of Korea

## Abstract

*Streptomyces avermitilis* produces clinically useful drugs such as avermectins and oligomycins. Its genome contains approximately 33 cytochrome P450 genes and they seem to play important roles in the biosynthesis of many secondary metabolites. The SAV\_7130 gene from *S. avermitilis* encodes CYP158A3. The amino acid sequence of this enzyme has high similarity with that of CYP158A2, a biflaviolin synthase from *S. coelicolor* A3(2). Recombinant *S. avermitilis* CYP158A3 was heterologously expressed and purified. It exhibited the typical P450 Soret peak at 447 nm in the reduced CO-bound form. Type I binding spectral changes were observed when CYP158A3 was titrated with myristic acid; however, no oxidative product was formed. An analog of flaviolin, 2-hydroxynaphthoquinone (2-OH NQ) displayed similar type I binding upon titration with purified CYP158A3. It underwent an enzymatic reaction forming dimerized product. A homology model of CYP158A3 was superimposed with the structure of CYP158A2, and the majority of structural elements aligned. These results suggest that CYP158A3 might be an orthologue of biflaviolin synthase, catalyzing C-C coupling reactions during pigment biosynthesis in *S. avermitilis*.

**Key Words:** P450, *Streptomyces avermitilis*, CYP158A3, Flaviolin, 2-Hydroxynaphthoquinone

## INTRODUCTION

*Streptomyces avermitilis* is a gram-positive soil-dwelling, filamentous actinobacterium. It has been of great pharmaceutical interest because it produces various useful drugs in human and veterinary medicine such as avermectins and oligomycins. The genome sequence of *S. avermitilis* was completed in 2003 and approximately 33 cytochrome P450 (P450) genes were found (Ikeda *et al.*, 2003). These P450 enzymes seem to play important roles in the biosynthesis of many secondary metabolites in *S. avermitilis*.

P450 enzymes are the major heme-containing catalysts involved in the oxidation of various substrates (Ortiz de Montellano, 2015). They are found in nearly all organisms, from bacteria to plants and mammals (Guengerich, 2008). Genome sequencing projects continue to reveal new genes for P450 enzymes from microorganisms including bacteria, archaea, and fungi. To date, more than 21,000 P450 genes have been

reported across all classes of organism (<http://drnelson.uthsc.edu/cytochromeP450.html/>) (Lee *et al.*, 2015; McLean *et al.*, 2015).

P450 enzymes from species in the genus *Streptomyces* are mainly integrated into biosynthetic operons for secondary metabolite pathways. These operons contain a series of enzymes for the production of an antibiotic, pigment, or some other secondary metabolite (McLean *et al.*, 2015). *S. coelicolor* is a prototypic *Streptomyces* strain; its genome has 18 P450-encoding genes. Our previous study reported that CYP105N1 from *S. coelicolor* is a P450 enzyme involved in the biosynthesis of coelibactin, which is a siderophore implicated in zinc-dependent antibiotic regulation (Lim *et al.*, 2012; McLean *et al.*, 2015).

Two CYP158A enzymes (CYP158A1 and CYP158A2) have been found in *S. coelicolor*. Previously, Zhao *et al.* (2005a, 2005b, 2007, 2012) reported that CYP158A1 and CYP158A2 produce polymers of flaviolin (biflaviolin or triflaviolin), which

**Open Access** <https://doi.org/10.4062/biomolther.2016.182>

This is an Open Access article distributed under the terms of the Creative Commons Attribution Non-Commercial License (<http://creativecommons.org/licenses/by-nc/4.0/>) which permits unrestricted non-commercial use, distribution, and reproduction in any medium, provided the original work is properly cited.

Received Aug 16, 2016 Revised Sep 22, 2016 Accepted Sep 22, 2016

Published Online Dec 13, 2016

**\*Corresponding Author**

E-mail: donghak@konkuk.ac.kr

Tel: +82-2-450-3366, Fax: +82-2-3436-5432

protect the bacterium in the soil from the deleterious effects of UV irradiation. In X-ray crystal structures of CYP158A1 and CYP158A2, two molecules of flavin were present in the closed active site (Zhao *et al.*, 2005a). The stacking of flavin molecules above the heme cofactor facilitates oxidative C-C coupling of the phenolic molecules to produce flavin dimers (Zhao *et al.*, 2005a). In the crystal structures of ferric CYP158A2, a substrate analogue, 2-hydroxy-1,4-naphthoquinone, was used and its catalytic activity was measured (Zhao *et al.*, 2005b).

The SAV\_7130 gene from *S. avermitilis* is located adjacent to a gene cluster for type III polyketide synthase, as is the gene encoding CYP158A2 in *S. coelicolor*; hence, these two proteins are likely to have a common function (Kelly *et al.*, 2005). SAV\_7130 encodes CYP158A3 and its amino acid sequence exhibits high similarity to that of CYP158A2. In this study, we examined the biochemical and enzymatic properties of recombinant *S. avermitilis* CYP158A3. Substrate binding titrations and 2-hydroxynaphthoquinone (2-OH NQ) dimerization experiments were performed to determine the reaction catalyzed by CYP158A3.

## MATERIALS AND METHODS

### Chemicals and enzymes

Glucose-6-phosphate, glucose-6-phosphate dehydrogenase, NADP<sup>+</sup>, and 2-OH NQ were purchased from Sigma (St. Louis, MO, USA). Isopropyl- $\beta$ -D-1-thiogalactopyranoside (IPTG) was purchased from Anatrace (Maumee, OH, USA). All the chemicals were of the highest grade commercially available.

### Construction of expression plasmids

Our general approach has been described previously (Lim *et al.*, 2012; Han *et al.*, 2015). The open reading frame for CYP158A3 was isolated directly by PCR amplification from *S. avermitilis* cells, and a 6 $\times$ His-C-terminal tag was appended using forward and reverse primers (5'CGAATCATATGACCGAGAAA3', 5'TCTAGACCGGAAGCTTTTAGTGATGGTGATG-GTGATGCCAGGTCACGGGCAG3'). The amplified fragment was cloned into a pCW(Or<sup>i</sup>) vector using the *Nde*I and *Xba*I restriction sites.

### Enzymes expression and purification

The expression and purification of CYP158A3 were carried out as previously described, with some modifications (Lim *et al.*, 2012; Park *et al.*, 2014). Briefly, *Escherichia coli* DH5 $\alpha$  cells transformed with pCW (CYP158A3) and pGroEL/ES vectors were inoculated in Luria-Bertani (LB) broth containing 50  $\mu$ g/mL ampicillin and 20  $\mu$ g/mL kanamycin; cells were then pre-cultured overnight at 37°C. LB cultures were then seeded into 500 mL of Terrific broth (TB) expression medium containing 50  $\mu$ g/mL ampicillin (1:100 dilution). The expression cultures were grown at 37°C, with shaking (220 rpm), until the optical density at 600 nm reached around 0.6 (Zhao *et al.*, 2007). Following supplementation (0.5 mM 5-aminolevulinic acid, 1.0 mM IPTG, 1.0 mM thiamine, and trace elements), the cultures were incubated for a further 22-24 h at 28°C, with shaking (190 rpm). The bacterial soluble fractions containing CYP158A3 were isolated and prepared from the TB expression cultures. CYP158A3 was purified using a Ni<sup>2+</sup>-NTA column (Qiagen, Valencia, CA, USA), as described previously

(Kim *et al.*, 2005; Park *et al.*, 2011). The dialyzed fraction was further concentrated using an Amicon Ultra-15 centrifugal filter unit (Millipore, Billerica, MA, USA) and dialyzed against 10 mM potassium phosphate buffer containing 10% glycerol.

### Spectroscopic characterization

Sodium dithionite was added to reduce the ferric-form purified CYP158A3. CO-ferrous CYP158A3 complexes were generated by passing CO gas through solutions of ferrous CYP158A3. The UV-visible spectra were collected on a CARY Varian spectrophotometer (Agilent Technologies, Santa Clara, CA, USA) in 100 mM potassium phosphate buffer (pH 7.4) at room temperature.

### Spectral binding titrations

Purified CYP158A3 was diluted to 1  $\mu$ M in 100 mM potassium phosphate buffer (pH 7.4) and divided equally into two glass cuvettes. The spectra were recorded between 350-500 nm on a CARY Varian spectrophotometer while titrating with ligands-myristic acid or 2-OH NQ (Yun *et al.*, 2005). The difference in absorbance between the maximum and minimum wavelength was plotted *versus* the substrate concentration (Schenkman *et al.*, 1967).

### P450 enzyme catalytic activity assay

Hydroxylation of 2-OH NQ by CYP158A3 was analyzed by LC-mass spectrometry. The reaction mixture contained 2 nmol purified CYP158A3 enzyme, and 200 mM *tert*-butyl hydroperoxide (tBHP) in 0.50 mL of 100 mM potassium phosphate buffer (pH 7.4), along with 400  $\mu$ M 2-OH NQ. Incubations were performed at 37°C for 1 h and terminated by adding 10  $\mu$ L 2N HCl; this was followed by ethyl acetate extraction (three times). The reaction products were recovered from the organic phase after drying under N<sub>2</sub>. Oxidized products were analyzed by LC-mass spectrometry on a Shimadzu LCMS-2010 EV system (Shimadzu, Kyoto, Japan), using LC-MS software. Products were separated on a Shim-pack VP-ODS column (2.0 mm i.d.  $\times$  250 mm; Shimadzu) at a flow rate of 1.0 mL/min. The mobile phase contained 90% solvent A (0.5% formic acid and 0.01% trifluoroacetic acid in water, v/v) followed by a linear gradient of solvent B (0.5% formic acid and 0.01% trifluoroacetic acid in acetonitrile, v/v), increasing to 100% solvent B over 20 min, and finally holding for 10 min with solvent B at a flow rate of 0.8 mL/min (Zhao *et al.*, 2005a). Mass spectra were recorded by electrospray ionization in negative mode to identify the metabolites. Interface and detector voltages were 4.4 kV and 1.5 kV, respectively. Nebulization gas flow was set to 1.5 mL/min. Interface, desolvation line, and heat block temperatures were 250°C, 230°C, and 200°C, respectively.

### Homology modeling of CYP158A3 protein

Homology modeling was performed on the Swiss-Model server (<https://swissmodel.expasy.org/>). CYP158A2 (PDB entry: 1T93) was used as a template for modeling. The resulting three-dimensional protein model was visualized in PyMOL (<http://www.pymol.org/>). The homology model was analyzed to identify possible substrate binding sites.

```

CYP15 8A3 MTEKTITEALPPVRHWPALNLTGVEFDPVLSQLMSEGPVSRIQLPNGEGWAWLVTR YDDVRMVANDPRF SRAAVMGRQVT
CYP15 8A2 MTEETISQAVPPVRDWPAVDLPGSDFDPLTELMREGPVTRISLPNGEGWAWLVTRHDDVRLVTNDPRFGREAVMDRQVT
***:***:***:***:***:***:***:***:***:***:***:***:***:***:***:***:***:***:***:***:***:***:***:***
CYP15 8A3 RLAPHFIP TAGAVGFLDPPDHTRLRRSVAAAF TARGVERVREKS RRMLDELI DELLRGGP PADLVETVLSPPPIAVVCEL
CYP15 8A2 RLAPHFIPARGAVGFLDPPDHTRLRRSVAAAF TARGVERVRERS RGMLDELVDAML RAGP PADL TEAVLSPPPIAVICEL
*****:*****:*****:*****:*****:*****:*****:*****:*****:*****:*****:*****:*****:*****:*****:*****:*****
CYP15 8A3 MGVP AADRHSMTWTQLILS SAHGAEVSEKARNDMGAHFERLIGERRGSTGEDVTS LLGAAVGS GEITLDEAVGLAVLIQ
CYP15 8A2 MGVPATDRHSMTWTQLILS SSHGAEVSEKARNEMNAYFSDLIGLRSD SAGEDVTS LLGAAVGRDEITLSEAVGLAVLLQ
*****:*****:*****:*****:*****:*****:*****:*****:*****:*****:*****:*****:*****:*****:*****:*****:*****
CYP15 8A3 IGGEAVTNNSGQLFYI LLTRPDLAERLRAEPKIRPQGIDELLY I PHRNAVGLSRIATED IEIRGVRI REGDTVYVSYLA
CYP15 8A2 IGGEAVTNNSGQMFHLLLSRPELAERLRSEPEIRPRAIDELLRW I PHRNAVGLSRI ALEDVEIKGVRI RAGDAVYVSYLA
*****:*****:*****:*****:*****:*****:*****:*****:*****:*****:*****:*****:*****:*****:*****:*****:*****
CYP15 8A3 ANRD PDVFPDPERIDLTRSPNPHV SFGF GPHYCVGSGMLARLESE LLVEALLDRVPGRLR LVAVPPGLVFPFKKGALIRGPEAL
CYP15 8A2 ANRD PEVFPDPRIDFERSPNPHV SFGF GPHYCPGSGMLARLESE LLVDAVLD RVPGLKLA VAPEDVFPFKKGALIRGPEAL
*****:*****:*****:*****:*****:*****:*****:*****:*****:*****:*****:*****:*****:*****:*****:*****:*****
CYP15 8A3 PVTW
CYP15 8A2 PVTW
****

```

**Fig. 1.** Sequence alignment of CYP158A3 and CYP158A2. These sequences share 81% identity. The residues corresponding to the conserved heme coordinated region are shown in box.

## RESULTS

### Amino acid sequence alignments for CYP158A3

The SAV\_7130 gene from *S. avermitilis* encodes a 404 amino acid enzyme, named CYP158A3 (<http://drnelson.uth-sc.edu/cytochromeP450.html/>). Its sequence contains both a heme-binding domain (FXGXGXXCXG) and an EXXR motif in the K-helix, which are conserved in P450 enzymes (Fig. 1). Amino acid sequence alignment of CYP158A3 from *S. avermitilis* with that of CYP158A2 from *S. coelicolor* shows high sequence identity (81%; Fig. 1) (Notredame *et al.*, 2000). The good sequence alignment to CYP158A2 suggests that the gene product of SAV\_7130 may be a biflavin synthase from *S. avermitilis* possessing flavin dimerization catalytic activity.

### Expression and purification of CYP158A3

Recombinant CYP158A3 protein was co-expressed with the molecular chaperones GroEL/ES in *E. coli*. The CO-reduced difference spectrum of *E. coli* cells transformed by pCW/158A3 expression vector (Fig. 2A) showed a typical P450 expression level of ~850 nmol P450 holoenzyme per liter of culture medium. CYP158A3 was purified by Ni<sup>2+</sup>-NTA affinity and size exclusion column chromatography. SDS-PAGE analysis showed a band with a size corresponding to that expected (45.1 kDa) from the open reading frame of the gene encoding CYP158A3, bearing a 6×His-tag (Fig. 2B). The absolute spectra of purified ferric-form CYP158A3 exhibited a Soret band at 416 nm, indicating a low-spin state; the distinctive  $\alpha$ - and  $\beta$ -bands of ferric P450 were observed at 588 nm and 534 nm, respectively (Fig. 2B).

### Binding analysis of CYP158A3

Binding titration analysis of CYP158A3 was performed to

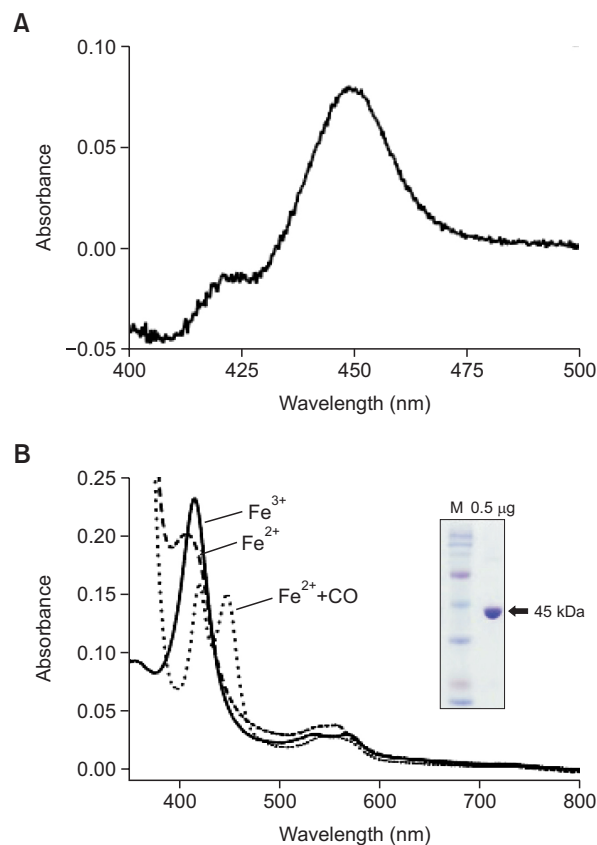


**Fig. 2.** Spectral analysis of CYP158A3. (A) Expression of recombinant CYP158A3 in *E. coli*. CO-binding spectra of CYP158A3 in *E. coli* whole cells were measured. (B) Absolute spectra of purified CYP158A3. The inset shows SDS-PAGE of the purified CYP158A3 protein.

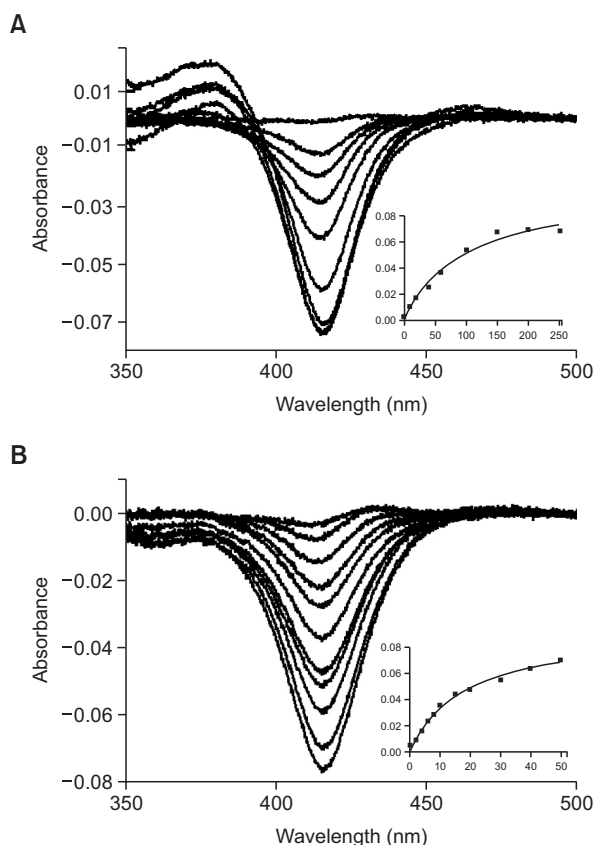


**Fig. 3.** Binding of myristic acid and 2-OH NQ to CYP158A3. (A) Binding titration of myristic acid to CYP158A3. The calculated  $K_d$  value for myristic acid was  $98 \pm 19 \mu\text{M}$ . (B) Binding titration of 2-OH NQ to CYP158A3. The calculated  $K_d$  value for 2-OH NQ was  $18 \pm 2 \mu\text{M}$ .

identify putative substrates. Titration of purified CYP158A3 with myristic acid produced a decrease at 416 nm and an increase at 378 nm, indicative of type I binding (Fig. 3A). The binding affinity ( $K_d$ ) of myristic acid was calculated to be  $98 \pm 19 \mu\text{M}$  (Fig. 3A). Since the substrate of CYP158A2, flavin, is not commercially available, its chemical analog, 2-hydroxynaphthoquinone (2-OH NQ), was used for the substrate binding analysis (Zhao *et al.*, 2005a). Titration with 2-OH NQ produced a decrease at 416 nm, however the spectral increase at 380 nm was not clear (Fig. 3B). The pseudo-type I binding titration results for CYP158A3 suggested that two molecules of 2-OH NQ might occupy the active site, consistent with a dimerization reaction. The calculated  $K_d$  value for 2-OH NQ was  $18 \pm 2 \mu\text{M}$  (Fig. 3B), indicating tight substrate binding. Additionally, resveratrol, stilbenes, and lauric acid displayed similar spectral changes upon binding; however, their binding affinities were not high (data not shown).

### Catalytic activities of CYP158A3

The catalytic activity of CYP158A3 towards 2-OH NQ was analyzed using LC-mass spectrometry. Purified CYP158A3 supported the catalytic turnover of 2-OH NQ, in the presence of tBHP, to yield the metabolic products displayed in the chromatogram (Fig. 4A). A total ion scan and selected ion monitoring mode scan for  $m/z=175$  were consistent with the inference

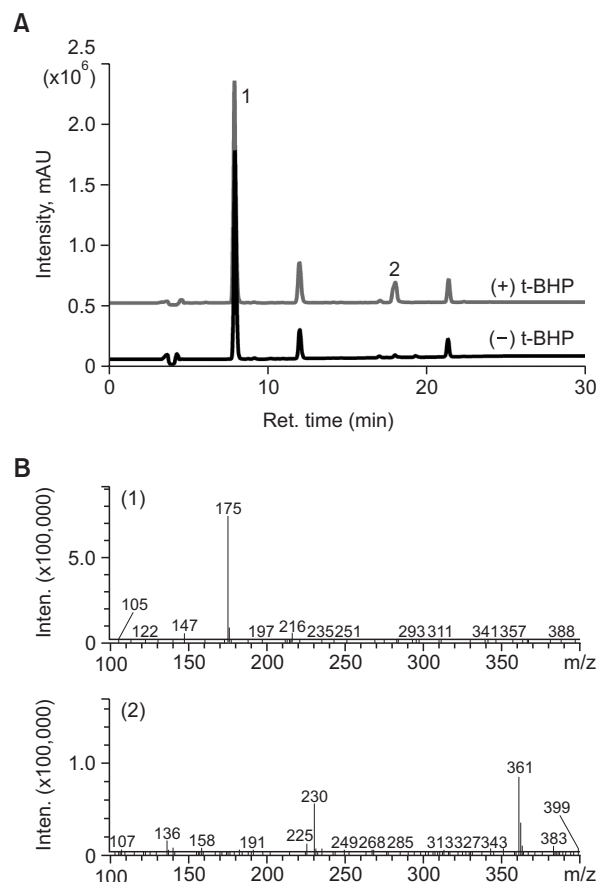


**Fig. 4.** LC-mass spectrometry analysis in the reaction of CYP158A3 with 2-OH NQ. (A) Hydroxylation of 2-OH NQ by CYP158A3 was performed in the presence and absence of tBHP. The substrate (2-OH NQ) (1) and a major product (2) were indicated, respectively. (B) MS scan of substrate (middle panel) and products (lower panel). The mass spectra of the reaction samples showed peaks at 7.8 min (substrate, 1) and 19.3 min (major product, 2). The  $m/z$  for  $[M]^+$  were 175 and 361 for the substrate and the product, respectively.

that the substrate peak at 7.8 min corresponded to 2-OH NQ (relative molecular mass: 174 Da) (Fig. 4B). The  $m/z$  of peak at 19.3 min indicated a mass of 361 Da, corresponding to the isomers of the dimeric form of 2-OH NQ after oxidation of the benzene ring (Fig. 4B). Dimeric isomers have not been definitively identified in the current analysis; further structural analysis will be required to define their detailed chemical structure.

### DISCUSSION

*S. avermitilis* was first isolated in Japan in 1979, and was screened by Merck Sharp & Dohme, resulting in the discovery of the avermectins, which are famous anthelmintic and insecticidal agents (Burg *et al.*, 1979; Demain, 1999). CYP171A1, a P450 enzyme encoded by the *aveE* gene from *S. avermitilis*, is involved in the biosynthesis of the avermectins, where it catalyzes the formation of the furan ring (Han *et al.*, 2016; Lamb *et al.*, 2003). Our previous effort to purify functional, recombinant CYP171A1 holoenzyme using an *E. coli* expres-



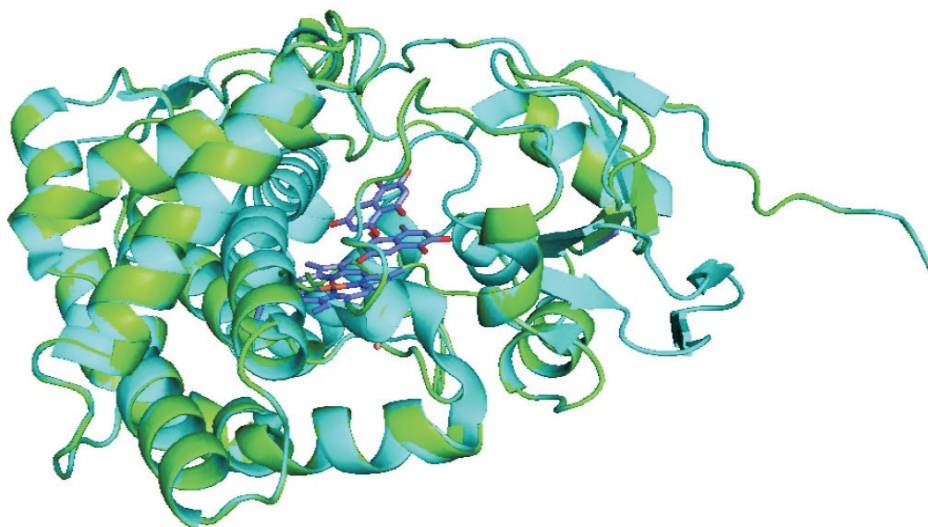


**Fig. 5.** Superimposed structures of CYP158A3 homology model and CYP158A2 crystal. The overall structure of the CYP158A3 homology model (green) was superimposed on the crystal structure of CYP158A2 (cyan; PDB entry: 1T93). CYP158A2 contains a heme group and two 2-OH NQ molecules at the active site.

sion system was not successful. Presumably, the bacterial expression system may not be optimal for the correct folding of recombinant CYP171A1.

For further analysis of the molecular structure, we tried to obtain the three-dimensional structure of CYP158A3. However, we were unable to produce crystals of CYP158A3 that diffracted well. To improve protein crystallization, a clone of CYP158A3 was constructed in which the first seven amino acids were truncated from the N-terminus. The truncated clone was expressed in *E. coli*. The truncation resulted in reduced expression (up to 74 nmol P450 per liter of culture). Nonetheless, highly concentrated pure protein could be obtained. However, the second crystallization attempt using this truncated CYP158A3 was not successful either as suitable crystals did not form.

To provide alternative structural information, a homology model of CYP158A3 was constructed using the crystal structure of CYP158A2 (PDB entry: 1T93) as a template (Fig. 5). Overall, the helical structure of the CYP158A2 homology model matched that of previously reported P450 enzymes (Fig. 5). When the model was superimposed on the crystal structure of CYP158A2, most residues from both structures aligned, implying that CYP158A3 may be a biflavin synthase in *S. avermitilis*.

The spectra for myristic acid and 2-HO NQ binding to purified CYP158A3 showed standard type I binding (Fig. 3). Previously, CYP158A2 displayed a similar type I spectral titration to 2-OH NQ with a  $K_d$  value of 43  $\mu\text{M}$  (Zhao *et al.*, 2005b). The calculated binding affinity of CYP158A3 in this study was a little stronger with a  $K_d$  value of 18  $\mu\text{M}$  (Fig. 3B). In our study, other aromatic compounds (resveratrol and stilbenes) also showed similar spectral changes associated with a type I binding mode (data not shown). Although the calculated binding affinities were not high, the type I binding patterns were clear, indicating that CYP158A3 may have an active site architecture suitable for compounds containing multiple aromatic rings. Meanwhile, an inhibitory type II binding mode was observed

during the binding titration with the azole compound, econazole, which had a  $K_d$  value of 0.2  $\mu\text{M}$  towards CYP158A3 (data not shown). Zhao *et al.* (2007) showed different binding modes and dimer forms of flaviolin produced by CYP158A1 biflavin synthase. In this study, the biflavin synthase activity of CYP158A3 also indicated the different dimer forms of 2-HO NQ (Fig. 4A). However, only a trace of enzyme activity was observed in the 2-OH NQ reaction of CYP158A3 (Fig. 4A) because 2-OH NQ lacking the 5- and 7-hydroxy groups create a more hydrophobic environment and disrupts the continuous water chain for proton delivery (Zhao *et al.*, 2005b).

In conclusion, recombinant *S. avermitilis* CYP158A3 was purified and its biochemical properties were characterized. The binding studies and enzymatic analyses suggested that CYP158A3 might be a biflavin synthase in *S. avermitilis*. The present findings will help elucidate the functional roles of P450 enzymes and provide biochemical insights into the complicated biosynthetic pathways of secondary metabolism in *Streptomyces* species.

## ACKNOWLEDGMENTS

This paper was supported by Konkuk University in 2014.

## REFERENCES

- Burg, R. W., Miller, B. M., Baker, E. E., Birnbaum, J., Currie, S. A., Hartman, R., Kong, Y. L., Monaghan, R. L., Olson, G., Putter, I., Tunac, J. B., Wallick, H., Stapley, E. O., Oiwa, R. and Omura, S. (1979) Avermectins, new family of potent anthelmintic agents: producing organism and fermentation. *Antimicrob. Agents Chemother.* **15**, 361-367.
- Demain, A. L. (1999) Pharmaceutically active secondary metabolites of microorganisms. *Appl. Microbiol. Biotechnol.* **52**, 455-463.
- Guengerich, F. P. (2008) Cytochrome p450 and chemical toxicology. *Chem. Res. Toxicol.* **21**, 70-83.

- Han, S., Pham, T. V., Kim, J. H., Lim, Y. R., Park, H. G., Cha, G. S., Yun, C. H., Chun, Y. J., Kang, L. W. and Kim, D. (2015) Functional characterization of CYP107W1 from *Streptomyces avermitilis* and biosynthesis of macrolide oligomycin A. *Arch. Biochem. Biophys.* **575**, 1-7.
- Han, S., Pham, T. V., Kim, J. H., Lim, Y. R., Park, H. G., Cha, G. S., Yun, C. H., Chun, Y. J., Kang, L. W. and Kim, D. (2016) Structural analysis of the *Streptomyces avermitilis* CYP107W1-oligomycin A complex and role of the tryptophan 178 residue. *Mol. Cells* **39**, 211-216.
- Ikeda, H., Ishikawa, J., Hanamoto, A., Shinose, M., Kikuchi, H., Shiba, T., Sakaki, Y., Hattori, M., and Omura, S. (2003) Complete genome sequence and comparative analysis of the industrial microorganism *Streptomyces avermitilis*. *Nat. Biotechnol.* **21**, 526-531.
- Kelly, S. L., Kelly, D. E., Jackson, C. J., Warrilow, A. G. S. and Lamb, D. C. (2005) The Diversity and Importance of Microbial Cytochrome P450. In *Cytochrome P450: Structure, Mechanism, and Biochemistry* (P. R. Ortiz de Montellano, Ed.), pp. 585-617. Plenum Press, New York.
- Kim, D., Wu, Z. L. and Guengerich, F. P. (2005) Analysis of coumarin 7-hydroxylation activity of cytochrome P450 2A6 using random mutagenesis. *J. Biol. Chem.* **280**, 40319-40327.
- Lamb, D. C., Ikeda, H., Nelson, D. R., Ishikawa, J., Skaug, T., Jackson, C., Omura, S., Waterman, M. R. and Kelly, S. L. (2003) Cytochrome p450 complement (CYPome) of the avermectin-producer *Streptomyces avermitilis* and comparison to that of *Streptomyces coelicolor* A3(2). *Biochem. Biophys. Res. Commun.* **307**, 610-619.
- Lee, G. Y., Kim, D. H., Kim, D., Ahn, T. and Yun, C. H. (2015) Functional characterization of steroid hydroxylase CYP106A1 derived from *Bacillus megaterium*. *Arch. Pharm. Res.* **38**, 98-107.
- Lim, Y. R., Hong, M. K., Kim, J. K., Doan, T. T., Kim, D. H., Yun, C. H., Chun, Y. J., Kang, L. W. and Kim, D. (2012) Crystal structure of cytochrome P450 CYP105N1 from *Streptomyces coelicolor*, an oxidase in the coelibactin siderophore biosynthetic pathway. *Arch. Biochem. Biophys.* **528**, 111-117.
- McLean, K. J., Leys, D. and Munro, A. W. (2015) Microbial Cytochromes P450. In *Cytochrome P450: Structure, Mechanism, and Biochemistry* (P. R. Ortiz de Montellano, Ed.), pp. 261-407. Springer, New York.
- Notredame, C., Higgins, D. G. and Heringa, J. (2000) T-Coffee: A novel method for fast and accurate multiple sequence alignment. *J. Mol. Biol.* **302**, 205-217.
- Ortiz de Montellano, P. R. (2015) *Cytochrome P450: Structure, Mechanism, and Biochemistry*. Springer, New York.
- Park, H. G., Lee, I. S., Chun, Y. J., Yun, C. H., Johnston, J. B., Montellano, P. R. and Kim, D. (2011) Heterologous expression and characterization of the sterol 14 $\alpha$ -demethylase CYP51F1 from *Candida albicans*. *Arch. Biochem. Biophys.* **509**, 9-15.
- Park, H. G., Lim, Y. R., Han, S. and Kim, D. (2014) Expression and characterization of truncated recombinant human cytochrome P450 2J2. *Toxicol. Res.* **30**, 33-38.
- Schenkman, J. B., Remmer, H. and Estabrook, R. W. (1967) Spectral studies of drug interaction with hepatic microsomal cytochrome P-450. *Mol. Pharmacol.* **3**, 113-123.
- Yun, C. H., Kim, K. H., Calcutt, M. W. and Guengerich, F. P. (2005) Kinetic analysis of oxidation of coumarins by human cytochrome P450 2A6. *J. Biol. Chem.* **280**, 12279-12291.
- Zhao, B., Bellamine, A., Lei, L. and Waterman, M. R. (2012) The role of Ile87 of CYP158A2 in oxidative coupling reaction. *Arch. Biochem. Biophys.* **518**, 127-132.
- Zhao, B., Guengerich, F. P., Bellamine, A., Lamb, D. C., Izumikawa, M., Lei, L., Podust, L. M., Sundaramoorthy, M., Kalaitzis, J. A., Reddy, L. M., Kelly, S. L., Moore, B. S., Stec, D., Voehler, M., Falck, J. R., Shimada, T. and Waterman, M. R. (2005a) Binding of two flavin substrate molecules, oxidative coupling, and crystal structure of *Streptomyces coelicolor* A3(2) cytochrome P450 158A2. *J. Biol. Chem.* **280**, 11599-11607.
- Zhao, B., Guengerich, F. P., Voehler, M. and Waterman, M. R. (2005b) Role of active site water molecules and substrate hydroxyl groups in oxygen activation by cytochrome P450 158A2: a new mechanism of proton transfer. *J. Biol. Chem.* **280**, 42188-42197.
- Zhao, B., Lamb, D. C., Lei, L., Kelly, S. L., Yuan, H., Hachey, D. L. and Waterman, M. R. (2007) Different binding modes of two flavin substrate molecules in cytochrome P450 158A1 (CYP158A1) compared to CYP158A2. *Biochemistry* **46**, 8725-8733.